



University for the Common Good

Effects of urban form and atmospheric stability on local microclimate

Drach, Patricia; Emmanuel, Rohinton

Publication date:
2015

Document Version
Peer reviewed version

[Link to publication in ResearchOnline](#)

Citation for published version (Harvard):
Drach, P & Emmanuel, R 2015, 'Effects of urban form and atmospheric stability on local microclimate'.

General rights

Copyright and moral rights for the publications made accessible in the public portal are retained by the authors and/or other copyright owners and it is a condition of accessing publications that users recognise and abide by the legal requirements associated with these rights.

Take down policy

If you believe that this document breaches copyright please view our takedown policy at <https://edshare.gcu.ac.uk/id/eprint/5179> for details of how to contact us.



Patricia
Drach

Effects of Urban Form and Atmospheric Stability on Local Microclimate

Patricia Drach¹, Rohinton Emmanuel²

¹ PROURB/FAU, Federal University of Rio de Janeiro, Cidade Universitária, Brazil, patricia.drach@gmail.com

² Department of Construction & Surveying, School of Engineering & Built Environment, Glasgow Caledonian University, Glasgow, UK,

dated: 8 June 2015

1. Introduction

The perspective of climate change increases the necessity of tackling the urban heat island (UHI) effects, by developing strategies to mitigate/adapt to changes. Although proper urban planning options could help minimize the effects of UHI, studies to adapt the built environment to these changes in urban areas are rare, particularly in the context of cool climate cities where urban warming is typically not seen as a current problem. This will change as the background climate continues to warm.

Analysing the influence of urban form on UHI could be a helpful way of reducing its negative consequences. While the exploration of the influence of urban form on local microclimate is helpful, it is necessary to untangle this effect from background atmospheric conditions that lead to such effects.

The present paper evaluates the effect of urban morphology (as measured by the Sky View Factor – SVF) on local climate according to atmospheric conditions exemplified by atmospheric stability - modified Pasquill-Gifford-Turner [PGT] classification system (Turner, 1970, modified by Mohan and Siddiqui, 1998) - in a cold climate city.

The increasingly urbanised nature of human habitation is contributing to develop worst scenarios. The intensity of climate change risks facing cities, which typically have compromised environmental conditions. Appropriate urban planning options could help ameliorate the heating problem and help "climate proof cities" for future climate change-related risks (Kleerekoper et al., 2012). In the context of cool climate cities, heat management (Stone et al., 2012) – both in terms of using the heat as a resource in winter and in terms of ameliorating its negative consequences in the summer – will be needed, in addition to climate change mitigation via greenhouse gas emission reduction. Nevertheless, the role of cities in climate change adaptation is only beginning to be addressed (for example: Hebbert and Jankovic, 2013) with city-specific urban climate change action plans remaining sketchy. In particular, urban form related studies to adapt to climate changes are rare (Shimoda, 2003).

In order to advance the importance of urban form manipulation to reduce the overheating risk it is necessary to explore the effectiveness of certain urban forms for this task and to clearly untangle the urban effect from the effect caused by atmospheric conditions. Krüger and Emmanuel (2013) estimated the effects of background atmospheric conditions on UHIs and intra-urban air temperature. They found that the range in intra-urban air temperature and relative warming at specific urban locations were accentuated after accounting for atmospheric stability. The relationship between the SVF and local warming was more pronounced under stable atmospheric conditions.

Given the increasing interest in climate change adaptation as well as the increasing use of models to evaluate the efficacy of various adaptation actions (cf. Tomlinson et al., 2012) such assessment should account for both the urban as well as background atmospheric effects on microclimates.

The present paper presents the effect of atmospheric conditions as exemplified by atmospheric stability (modified Pasquill-Gifford-Turner classification system) and urban morphology as measured by the Sky View Factor (SVF) on intra-urban variations in air temperature in a cold climate city, in and around the mature urban area of Glasgow, UK (55° 51' 57.294"N, 4° 15' 0.2628"W). The aim is to highlight their relative importance and to make preliminary explorations of the local warming effect of urban morphology under specific atmospheric stability classes.

Forty-nine locations were selected in the city centre, on the basis of SVF to represent a wide variety of urban forms (narrow streets, neighbourhood green spaces, urban parks, typical street canyons and public squares) and seven of these were assigned as locations for fixed weather stations. Thirty-one temperature measurement campaigns were made, using a 'traverse' method on a 'Meteobike' and on foot. The locations were chosen to represent a variety of urban formation (narrow streets, neighborhood greenspaces, urban parks, uniform and non-uniform street canyons and public squares). The visualization of local temperature variations was accomplished using Arc-Map tool from Arc-GIS package.

The present work indicates that the maximum intra-urban temperature differences (i.e. temperature difference between the coolest and the warmest spots in a given urban region) is strongly correlated with atmospheric stability. It appears that atmospheric stability has larger effect on intra-urban temperature variations than urban morphology in a cold climate city. The combined effect of the two provides interesting variations in local

temperatures that may have urban planning implications, especially as the background climate continues to warm.

2. Methods and materials

The present study involved three specific tasks: the classification of atmospheric stability, determination of urban morphology and local temperature variations. Local temperature was measured at fixed locations as well as using a mobile traverse.

2.1 Atmospheric stability

The Pasquill-Gifford-Turner (PGT) (Table 1) classification system (Turner, 1970, modified by Mohan and Siddiqui, 1998) was adopted and the data was obtained from a weather station (Davis Vantage Pro2) in the Glasgow city centre (55° 51' 57.294"N, 4° 15' 0.2628"W, 138m amsl – see Table 2 for details) to classify atmospheric stability.

Table 1 Atmospheric stability classes PGT (changed after Mohan and Siddiqui, 1998)

| WS (m/s) | Daytime SR (W/m ²) | | | Night time CC (octas) | | | |
|----------|--------------------------------|------------------|------------------|-----------------------|------------------|------------------|-------------------|
| | High ¹ | Mod ² | Low ³ | Cloudy | Low ⁴ | Mod ⁵ | High ⁶ |
| ≤2 | A | A-B | B | C | G-F | F | D |
| 2-3 | A-B | B | C | C | F | E | D |
| 3-5 | B | B-C | C | C | E | D | D |
| 5-6 | C | C-D | D | D | D | D | D |
| >6 | C | D | D | D | D | D | D |

Legend: WS wind speed, SR global solar radiation, CC cloud cover, ¹ (>600), ² (300-600), ³ (<300), ⁴ (0-3), ⁵ (4-7), ⁶ (8), A (highly unstable or convective), B (moderately unstable), C (slightly unstable), D (neutral), E (moderately stable), and F (extremely stable), G (extremely stable, low wind).

Table 2 Glasgow Caledonian University Weather Station (1s)

| Coordinates and SVF | Fish-eye photo | Black and white mask | Solar path |
|--|--|---|--|
| Latitude: 55° 51' 57.294"N and Longitude: 4° 15' 0.2628"W |  |  |  |
| SVF 0.774 | | | |



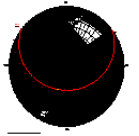


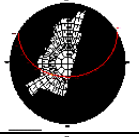

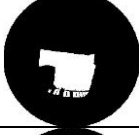



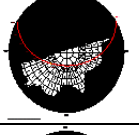
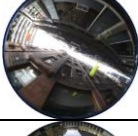

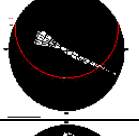


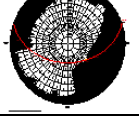
2.2 Urban morphology

The determination of urban morphology was based on the Sky View Factor (SVF) computed by RayMan Pro (Matzarakis et al. 2007, Matzarakis et al. 2010). The images were taken by using fisheye-lenses photographs (SIGMA 4.5mm f 2.8 EX). 49 locations representing a wide variety of urban formation (narrow streets, neighbourhood greenspaces, urban parks, uniform and non-uniform street canyons and public squares) were selected on the basis of SVF and seven of these were assigned as locations for fixed weather stations (see Table 3 for details). Figure 1 shows the location of all selected measurement points and the routes in three directions (east, central, west) which were defined to access all 42 points as fast as possible.



Fig. 1 Measurement point locations in Glasgow City Centre

Table 3. Location of the seven stationary points (2s ... 7s)

| Coordinates and SVF | Fish-eye photo | Black and white mask | Solar path |
|--|--|---|--|
| Blythwood Square (POINT 2s) Latitude: 55° 51' 48.7542"N / Longitude: 4° 15' 44.1288"W SVF: 0.017 |  |  |  |
| City Council – Hope St (POINT 3s) Latitude: 55° 51' 31.8744"N / Longitude: 4° 15' 33.0804"W SVF: 0.201 |  |  |  |
| City Council – Montrose St (POINT 4s) Latitude: 55° 51' 37.875"N / Longitude: 4° 14' 46.4274"W SVF: 0.127 |  |  |  |
| City Council - Elmbank St (POINT 5s) Latitude: 55° 51' 48.618"N / Longitude: 4° 16' 3.9144"W SVF: 0.205 |  |  |  |
| Lighthouse – Mitchell Ln (POINT 6s) Latitude: 55° 51' 35.445"N / Longitude: 4° 15' 20.1132"W SVF = 0.042 |  |  |  |
| St Andrew's Cathedral (POINT 7s) Latitude: 55° 51' 20.5122"N / Longitude: 4° 15' 8.7762"W SVF = 0.440 |  |  |  |

2.3 Mobile temperature measurement protocol

Thirty-one temperature measurement campaigns were made during Spring and Summer 2013. In order to cover a large area of city centre within a relatively short time we used the 'traverse' method on three pre-determined routes (Figure 1), using a Tandem Recumbent Zöhrer model called a 'Meteobike' (Figure 2) and on foot.



Fig. 2. Meteobike

All three routes started at Point 25 and ended at Point 10 (Figure 1) and spent two minutes at each measurement point. The first four measurements at each point were discarded to allow the data logger to stabilise. At a measurement interval of 10 seconds this gave eight measurements for each point which were then averaged. Measurement campaigns began at 2:30 p.m. local time (to be closer to the daily maximum temperature which typically occurred at 3:00 p.m. local time) and lasted approximately an hour. The loggers characteristics of the weather station (WS) and data loggers (Tinytag TGP-4500) are shown in Table 4. They were housed in radiation shields (ACS-5050 - Stevenson Type Screen) to prevent direct and diffuse solar radiation falling on them.

Table 4. Characteristics of the weather station (WS) and data loggers (Tinytag TGP-4500)

| Sensor | Position | Resolution | Range | Accuracy |
|------------------------------------|---|--------------------------------|----------------|----------------------------|
| Air temperature (WS) | Reference weather station | 0,1°C ou 1°C (user-selectable) | -40° to +65°C | ±0,5°C |
| Air humidity (WS) | Reference weather station | 1% | 1 to 100% | ±3% (0-90%), ±4% (90-100%) |
| Wind velocity (WS) | Reference weather station | 0,4 m/s | 1 to 80 m/s | ±1 m/s |
| Wind direction (WS) | Reference weather station | 22,5° | 0 - 360° | ±3° |
| Solar radiation (WS) | Reference weather station | 1 W/m2 | 0 to 1800 W/m2 | ±5% |
| Air temperature (Tinytag TGP-4500) | Traverses by bike or by foot and fixed points | 0,01°C | -25°C a +85°C | ±0,45°C |

2.3 Spatial representation of temperature variations

Measurement points were geo-referenced using a handheld GPS (GPS Garmin MAP). These were then transferred to a GIS map (ArcGIS v. 10.1) which itself was a combination of 2D (Lidar map, [Edinburgh University, 2013](#)) and 3D (Vector map, [Landmap Spatial Discovery, 2013](#)). Figure 3(a) and (b) shows these maps respectively.

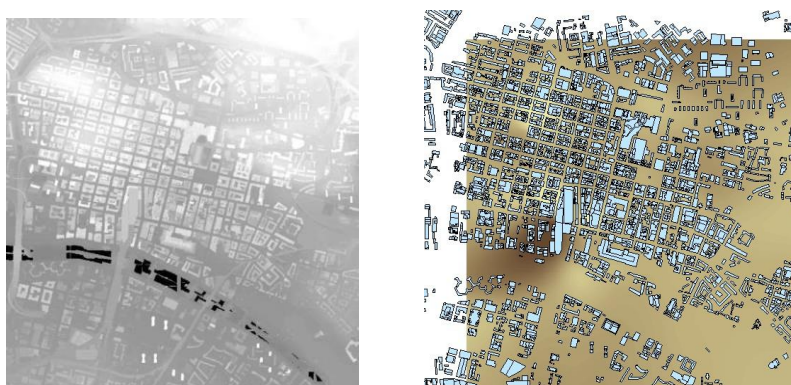


Fig 3. (a) Lidar map of Glasgow city centre and (b) Vector map (blocks) with soil map

The visualization of local temperature variations was accomplished using Arc-Map tool from Arc-GIS package. Figure 4 shows the temperature values for July, 19th 2013 and the sky view factor (SVF) for each measurement spot.

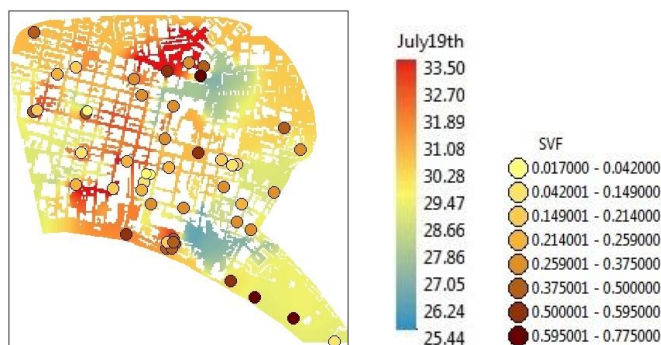


Fig 4. Air temperature variations in July 19th 2013 and the SVF

The relationship between the SVF values to the air temperatures in urban areas tends to present a parabolic behaviour. Extreme SVF values were associated with higher and lower temperatures.

3. Results

In order to investigate the influence of atmospheric stability on local temperature, each measurement campaign was classified into relevant PGT Class (see Table 1 for the classification system). First results appeared inconclusive. Classes A-B and B exhibit the expected parabolic relationship (i.e. lower temperatures at very open – i.e. green and highly built-up i.e. shaded sites) during the day. However, this appears not the case with atmospheric stability classes A and C. The situation is similar when the variations on a very hot day (Jul 19th; maximum temperature difference with respect to the reference station = 7.70°C) and a cold day (May 10th; maximum temperature difference = 2.02°C) (see Figure 5).

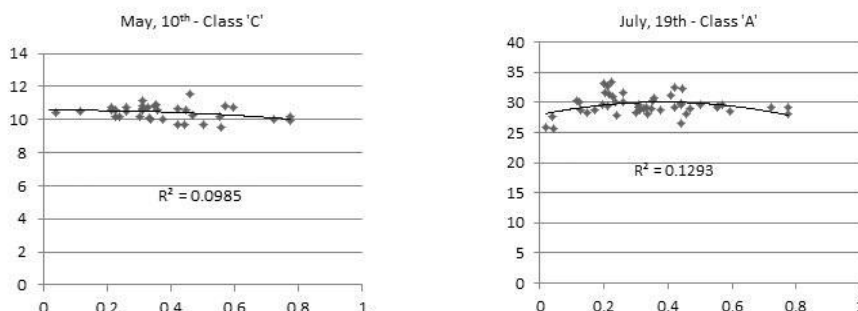


Fig 5. Temperature-SVF relationship on (a) coldest [Class 'C'] and (b) hottest [Class A] days

However, the maximum temperature difference between the traverse points varied widely across the measurement campaigns (see Table 5). These differences (termed here as intra-urban temperature differences) varied between 1.96-7.70°C.

Table 5. Maximum intra-urban temperature differences on measurement days

| Day | Class | Temperature difference | Day | Class | Temperature difference |
|-----------|-------|------------------------|-------------|-------|------------------------|
| May, 8th | C | 2.35 | June 18th | A-B | 5.56 |
| May 9th | C | 2.29 | June 19th | B | 7.38 |
| May 10th | C | 2.02 | June 25th | B | 3.47 |
| May 20th | B | 4.84 | June 26th | A-B | 6.45 |
| May 21th | A | 7.20 | June 27th | B | 3.76 |
| May 22th | A-B | 4.99 | July 1st | B | 4.35 |
| May 28th | C | 1.96 | July 3rd | C | 3.28 |
| May 29th | B | 2.56 | July 9th | C | 3.28 |
| May 30th | A-B | 5.33 | July 10th | A-B | 3.25 |
| June 5th | A-B | 4.80 | July 11th | A-B | 2.89 |
| June 6th | A-B | 5.17 | July 18th | A | 7.05 |
| June 7th | A-B | 7.61 | July 19th | A | 7.70 |
| June 10th | B | 4.36 | July 22th | A-B | 4.71 |
| June 11th | B-C | 5.96 | August 13th | A-B | 6.64 |
| June 12th | B | 4.26 | August 14th | C | 3.68 |
| June 17th | A-B | 4.19 | | | |

Figure 6 shows the relationship between maximum intra-urban temperature differences (°C) and atmospheric stability.

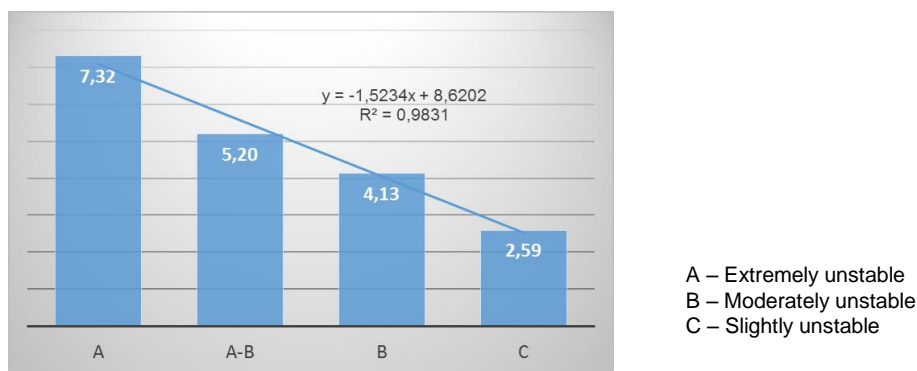


Fig 6. Maximum intra-urban temperatures vs. atmospheric stability

Here it is possible to observe that the presence of a highly unstable class ('A') is associated with the largest intra-urban temperature differences in Glasgow city centre. The more unstable the atmosphere the larger the intra-urban temperature variation. A high correlation between atmospheric class and air temperature difference can be noticed - $R^2 = 0.98$.

Table 6. presents average intra-urban temperature differences by atmospheric stability classes in scatter plot.

Table 6. Distribution of temperature differences according to atmospheric stability classes

| Atmospheric Stability Class (PGT) | A | A-B | B | C |
|---|---|-----|---|---|
| Average temperature difference (°C) vs. Sky View Factor | | | | |

Relationship between SVF and intra-urban temperature differences are similar across all atmospheric stability classes (Range of $R^2 = 0.4031 - 0.4308$).

5. Discussion and conclusions

The present work indicates that the maximum intra-urban temperature differences (i.e. temperature difference between the coolest and the warmest spots in a given urban region) is strongly correlated with atmospheric stability. It appears that atmospheric stability has larger effect on intra-urban temperature variations than urban morphology in a cold climate city. The combined effect of the two provides interesting variations in local temperatures that may have urban planning implications, especially as the background climate continues to warm.

The relationship between urban morphology (as measured by the SVF) and urban temperature variations, while being one of the most well-studied aspect of UHI research, is not so clear. Atmospheric stability as defined by the PGT system, has an effect on the relationship between SVF and temperature but this relationship too needs additional clarification. SVF appears to have a 'parabolic' relationship with air temperature during daytime (both very open – green sites as well as heavily built up – shaded sites show lower temperatures), but this relationship is not conclusive. The more unstable atmospheric stability classes have the largest variations in urban temperatures while the less unstable classes exhibit smaller variations. All of the classes explain about half of the variations in urban temperatures. The spatial patterns in local temperature variations consistently show that water bodies and urban parks have consistently lower temperature variations. Thus, greenery and urban materials could play an important role in influencing the local climate in cold cities.

Knowing this limitation of urban morphology's influence on local temperature variations could be useful in devising realistic planning/design strategies to ameliorate urban overheating in the coming years as the background climate continues to warm.

Acknowledgment

We gratefully acknowledge the financial help provided by the Brazilian funding agency CNPq (National Council for Scientific and Technological Development, Brazil Science without Borders 246551/2012-7) and facilities, instrumentation and analysis provided by the School of Engineering and Built Environment at Glasgow Caledonian University.

References

- Edinburgh University, School of Informatics. URL <<http://data.inf.ed.ac.uk/geo/lidar/>> (accessed 06.15.13).
- Hebbert M., Jankovic V. 2013. Cities and climate change: the precedents and why they matter. *Urban Studies*, 50, 1332-1347.
- Kleerekoper L., van Esch M., Salcedo T. B. 2012. How to make a city climate-proof, addressing the urban heat island effect. *Resources, Conservation and Recycling*, 64, 30–38.
- Krüger E., Emmanuel R. 2013. Accounting for atmospheric stability conditions in Urban Heat Island studies: the case of Glasgow, UK. *Landscape and Urban Planning*, 117, 112-121.
- Matzarakis A, Rutz F, Mayer H. 2007. Modelling radiation fluxes in simple and complex environments - Application of the RayMan model. *International Journal of Biometeorology*, 51, 323–34.
- Matzarakis A, Rutz F, Mayer H. 2010. Modelling radiation fluxes in simple and complex environments: basics of the RayMan model. *International Journal of Biometeorology*, 54(2), 131–139.
- Mohan M., Siddiqui T. A. 1998. Analysis of various schemes for the estimation of atmospheric stability classification. *Atmospheric Environment*, 32(21), 3775-3781.
- Shimoda Y. 2003. Adaptation measures for climate change and the urban heat island in Japan's built environment. *Building Research and Information*, 31, 222-230.
- Tomlinson C. J., Chapman L., Thornes J. E., Baker C. J. 2012. Derivation of Birmingham's summer surface urban heat island from MODIS satellite images. *International Journal of Climatology*, 32, 214–224.
- Turner D. B. 1970. Workbook of atmospheric dispersion estimates. Office of Air Program Pub. No. AP-26, Environmental Protection Agency, USA.